



Contents lists available at ScienceDirect

Spectrochimica Acta Part A: Molecular and Biomolecular Spectroscopy

journal homepage: www.elsevier.com/locate/saa

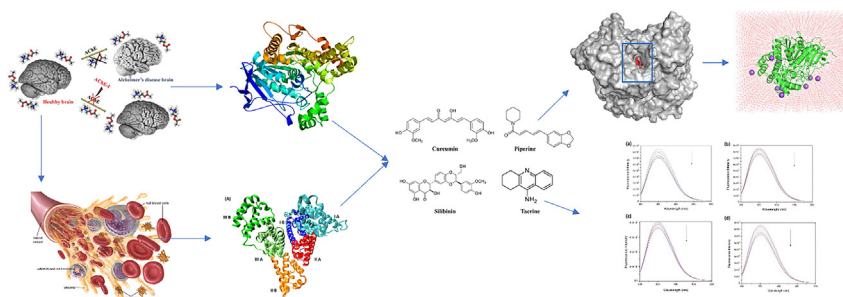
Binding studies of known molecules with acetylcholinesterase and bovine serum albumin: A comparative view

Kandasamy Saravanan^{a,b,*}, Subramani Karthikeyan^c, Srinivasan Sugarthi^d, Arputharaj David Stephen^e^a Faculty of Chemistry, University of Warsaw, Ludwika Pasteura 1, Warsaw 02093, Poland^b Department of Physics, Periyar University, Salem 636 011, India^c G. S. Gill Research Institute, Guru Nanak College (Autonomous), Chennai 600 042, India^d Department of Physics and Nanotechnology, SRM Institute of Science and Technology, Kattankulathur 603203, India^e Department of Physics, PSG College of Arts and Science, Coimbatore 641014, India

HIGHLIGHTS

- The fluorescence and molecular docking confirm the strong interactions.
- MD confirms the stability of the molecule in the active site of BSA and AChE.
- NCI approach visualizes the intermolecular interactions in protein-ligand complexes.

GRAPHICAL ABSTRACT



ARTICLE INFO

Article history:

Received 20 January 2021

Received in revised form 25 March 2021

Accepted 15 April 2021

Available online 19 April 2021

Keywords:

Interaction study

Steady-state spectroscopy analysis

Molecular docking

MD simulation and binding Free energy

NCI analysis

ABSTRACT

The interactions between selected molecules (piperine, tacrine, curcumin and silibinin) and proteins (acetylcholinesterase and bovine serum albumin) were investigated by Fluorescence spectroscopy, molecular docking, molecular dynamics, free energy calculation and non-covalent interaction analysis. These binding characteristics are of huge interest for understanding pharmacokinetic mechanism of the target molecules. The steady-state emission spectrum results showed that presence of static quenching mode for piperine, tacrine, curcumin, silibinin molecules with BSA and AChE complexes separately and this excitation-emission matrix analysis suggest that formation of ground-state complex between piperine, tacrine, curcumin, silibinin drugs and both BSA, AChE protein molecules. And, the binding model from molecular docking analysis of both BSA and AChE with these molecules clearly displayed non-covalent interactions (hydrogen bonding and hydrophobic interactions) which played a significant role in the binding mechanism. Further, the protein-ligand complexes are subjected to molecular dynamics and binding free energy calculation to confirm the stability of the molecule in the active site of BSA and AChE. The NCI (non-covalent interaction) approach supports to visualize the iso-surface of the reduced density gradient of such interactions between protein and ligands.

© 2021 Elsevier B.V. All rights reserved.

* Corresponding author at: Faculty of Chemistry, University of Warsaw, Poland.

E-mail addresses: saravanansmtr@gmail.com, s.kandasamy@uw.edu.pl (K. Saravanan).

1. Introduction

Alzheimer's disease (AD) is called senile dementia which is an age-related progressive neurodegenerative brain disorder. Notably, resulting in loss of memory and cognitive functions, the decline in language-related skills and behavioral disturbances. Moreover, AD

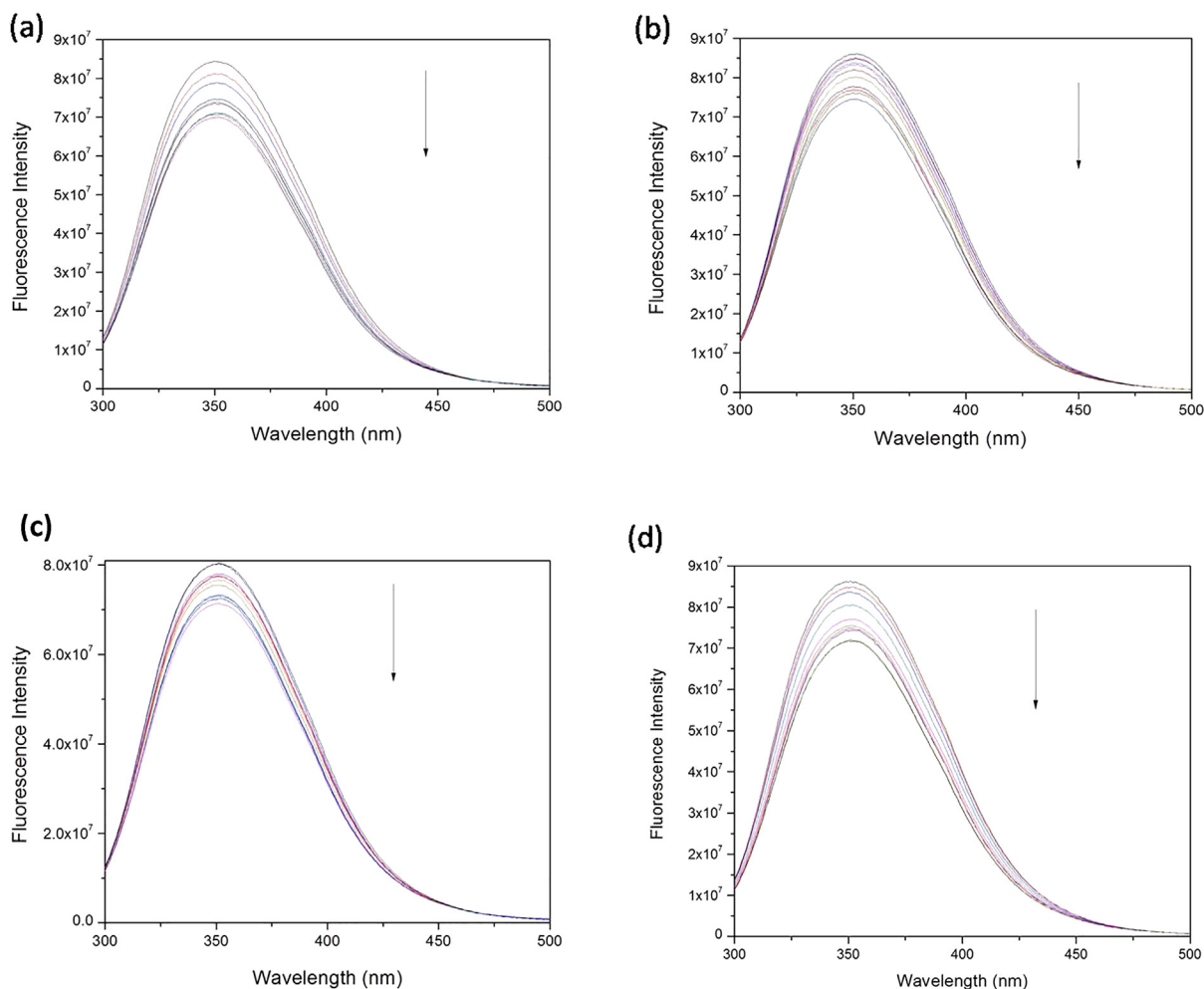


Fig. 1. Steady state emission spectrum of BSA with (a) Piperine (b) Tacrine (c) Curcumin (d) Silibinin complexes (BSA concentration is $10\ \mu\text{M}$ and drug concentration (a) piperine ($0\text{--}10\ \mu\text{M}$) (b) tacrine ($0\text{--}12\ \mu\text{M}$) (c) curcumin ($0\text{--}10\ \mu\text{M}$) (d) silibinin ($0\text{--}8\ \mu\text{M}$) with $1\ \mu\text{M}$ interval).

is the 4th leading cause of death in the world, over 40 million people affected by AD [1]. Therefore, AD is considered the most common neurodegenerative disorder and a major health concern to societies worldwide [2]. Currently, there is no successful treatment; however, acetylcholinesterase inhibitors control the progression of AD. Due to the exerts of non-cholinergic functions with the nervous system, Acetylcholinesterase (AChE) is hydrolyzing the neurotransmitter acetylcholine that leads to the molecular mechanism of pathogenesis of Alzheimer's disease. It can reduce this abnormal activity of the enzyme with the help of potential activity inhibitors. It mainly aims this present computational study to understand the deeper structural and binding mechanism of AChE with selected inhibitors. The clear active site details of AChE are mandatory to confirm the new inhibitor design. Based on the reports, the active site contains different sub-sites, such as the catalytic triad; an oxyanion hole; an acyl binding pocket; an anionic binding site; and a peripheral anionic binding site which is detected at the bottom of narrow gorge ($20\ \text{\AA}$). To discover the AChE-inhibiting small molecules from herbal plants, we have screened biologically active compounds traditionally. The scientific reports show that the natural products (polyphenols, flavonoids, vitamins, alkaloids, carbamates, carotenes and lycopenes) exhibit several biological properties. To date, AChE is the important enzyme target for the pharmacological treatment of AD [3–8]. There are three plant-derived (galantamine, huperzine A &

rivastigmine) and two synthetic (donepezil & tacrine) drugs available in the market for the treatment of AD. Importantly, these all drugs are AChE inhibitors which also does not cure the disease completely.

Serum albumins are the most abundant carrier proteins of the circulatory system in human beings which exhibits several physiological functions. The most important properties of these proteins involved in the transport and distribution of many molecules like fatty acids, amino acids, hormones, cations, anions, many diverse drugs and other organic compounds. Among the serum albumins, the Bovine serum albumin (BSA) is one of the most extensively studies protein; especially the structural homology of the BSA is highly similar to human serum albumin (HSA) which contains three homologous domains (I, II, III) with disulfide bonds. Interestingly, BSA contains two tryptophan residues (Trp-134 in the first domain and Trp-213 in the second domain) that carries intrinsic fluorescence [9–11]. This is the only reason that fluorescence quenching can measure the binding affinities of BSA with different ligand molecules. It is important to study the interactions of ligands with this protein [12,13].

To study the reactivity of chemical and biological systems in low concentration and under physiological conditions, Fluorescence spectroscopy is a non-intrusive measurement [14]. Quenching measurements can reveal the accessibility of quenchers to fluorophores to understand the binding nature of BSA and

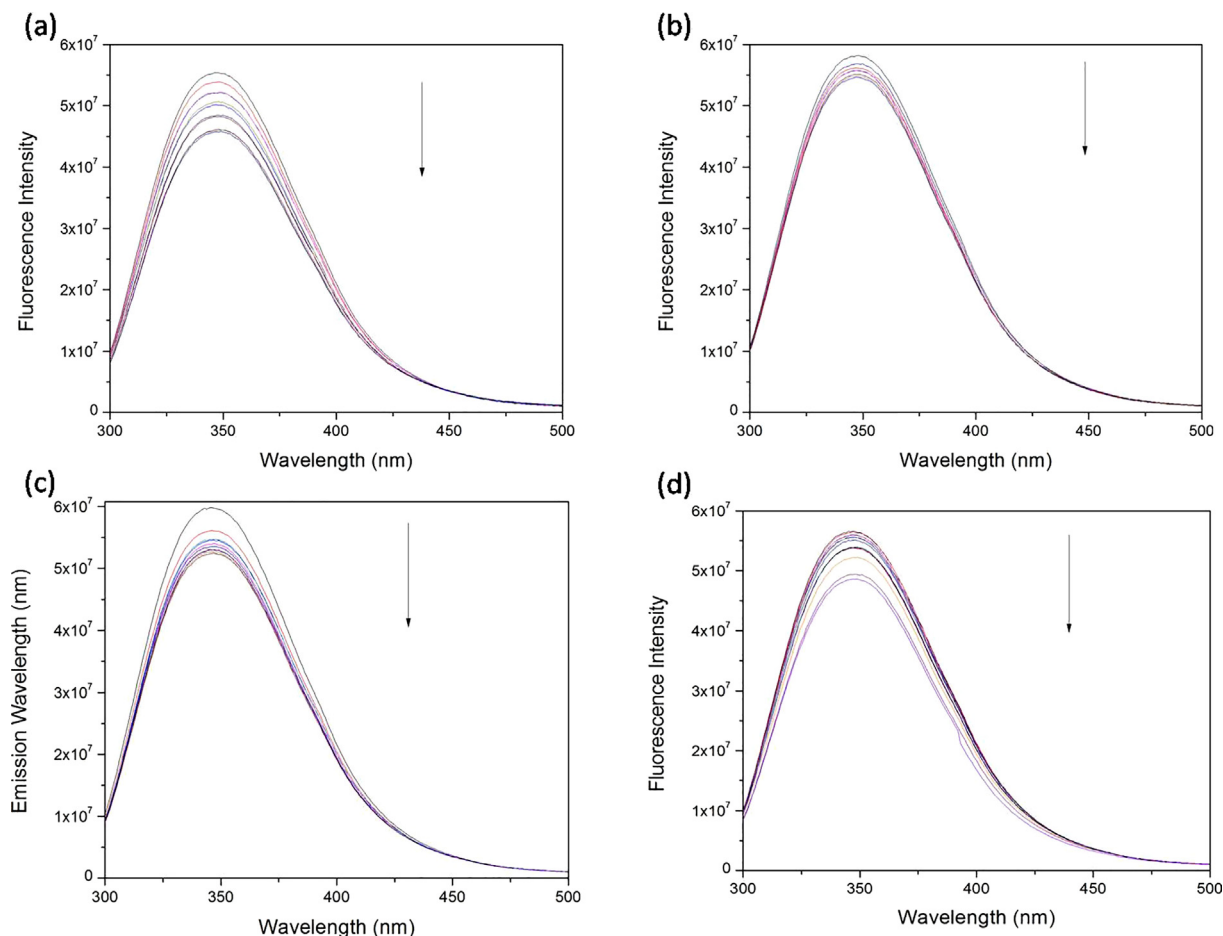


Fig. 2. Steady state emission spectrum of AChE with (a) Piperine (b) Tacrine (c) Curcumin (d) Silibinin complexes (AChE is 10 μM kept as constant and the drug concentration varies (a) piperine (0–2 μM) (b) tacrine (0–1 μM) (c) curcumin (0–1 μM) (d) silibinin (0–4 μM) with 0.2 μM interval).

Table 1
Fluorescence binding Parameters for all four compounds in BSA and AChE complexes (pH=7.4).

Proteins	Compounds	$K_q (\times 10^{18} \text{L mol}^{-1} \text{s}^{-1})$	$K_b (\times 10^5 \text{L/mol})$	n
BSA	Piperine	0.0018	1.16	0.96
	Tacrine	6.2831	2.57	0.86
	Curcumin	5.5184	1.78	0.93
	Silibinin	0.1401	4.57	1.12
AChE	Piperine	0.1404	1.67	0.95
	Tacrine	0.1079	0.69	0.93
	Curcumin	0.0019	0.48	1.05
	Silibinin	2.1200	3.05	0.82

AChE with different ligand molecules. Nowadays, researchers are interested to study natural compounds with different enzymes/proteins/receptors because of several beneficial biological effects. These spectroscopic and computational studies also focused on three natural compounds (curcumin, piperine and Silibinin) that are traditionally believed to offer cognitive benefits. Piperine is bioactive alkaloids, existing in the black pepper; curcumin is a polyphenolic compound, occurred in the turmeric; silibinin is also a natural polyphenolic flavonoid, found in milk thistle and tacrine is a synthesized Alzheimer drug [AChE inhibitor]. All the compounds exhibit an anti-oxidant, anti-inflammation, anti-cancer and anti-Alzheimer properties [15–18].

The present spectroscopic and computational report deals with the mechanism of binding of ligand with AChE and BSA by fluorescence steady-state measurements, molecular docking, molecular dynamics, free energy calculation and NCI analysis. Notably, the

AChE inhibition assay of all the selected molecules was already reported [19–21] and computational studies (DFT, molecular docking, molecular dynamics, free energy calculation and QM/MM based charge density analysis) of curcumin and piperine were reported by Saravanan et al [22,23]. Therefore, we also conducted spectroscopic analysis and *in silico* analysis of all the selected molecules with AChE/BSA to support the already reports.

2. Material and methods

2.1. Materials and sample preparation

The Acetylcholinesterase (AChE, C3389), Bovine Serum Albumin (BSA, A2058/ Fraction V), Curcumin (C1386), Piperine (P49007), Silibinin (S0417) and 9-Amino-1,2,3,4-tetrahydroacridine hydrochloride hydrate (Tacrine, A3773) purchased in Sigma

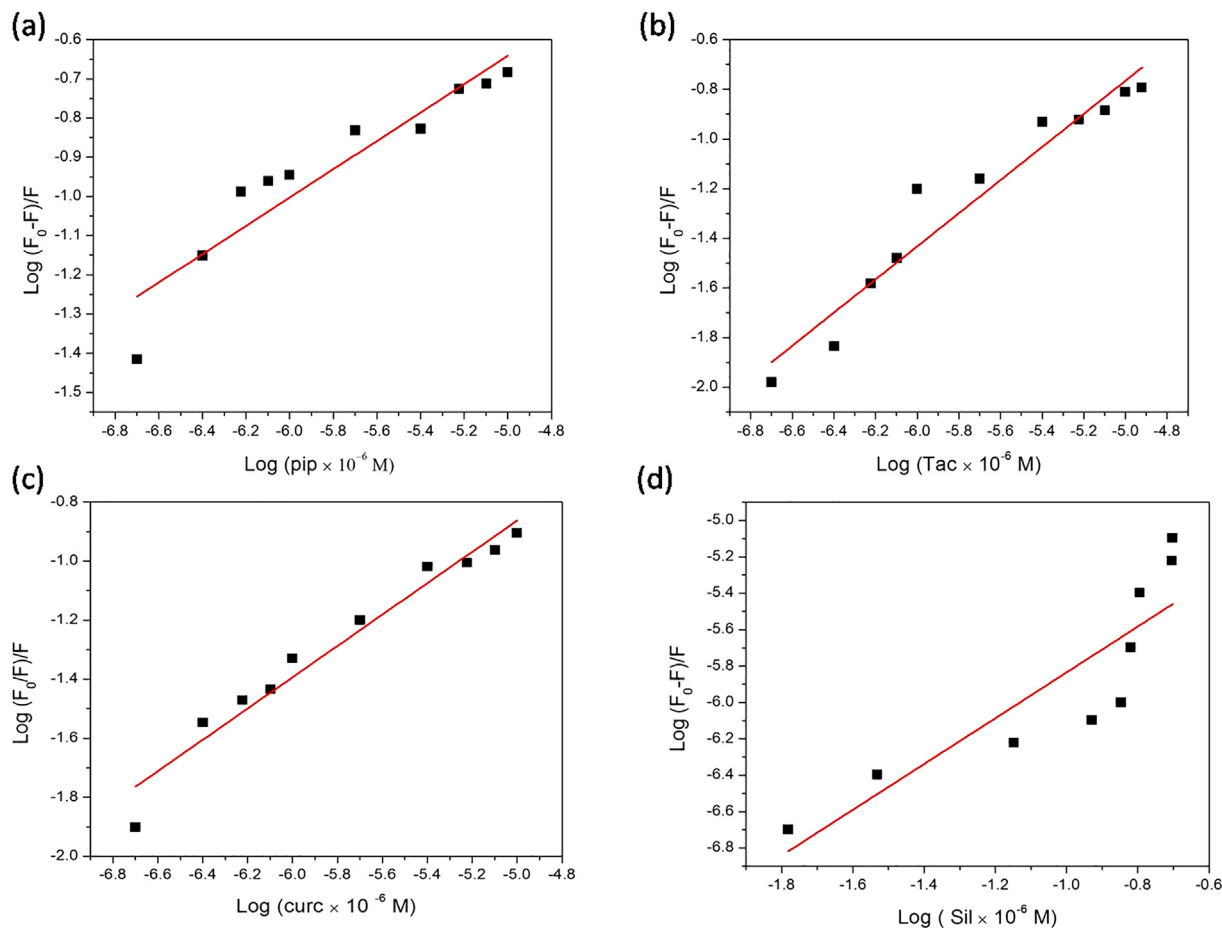


Fig. 3. Log plot of BSA with (a) Piperine (b) Tacrine (c) Curcumin (d) Silibinin complexes.

Aldrich. We verified the purity of samples using UV–vis absorption spectroscopy, and the purity of the samples was over 97%. The stock solution of AChE and BSA was prepared by using a phosphate buffer solution at pH 7.4. Similarly, the stock solution of selected ligand molecules was prepared in ethanol (%) and then diluted in the same buffer solution (phosphate buffer solution at pH 7.4) with no further purification. Because of this solvent effect, there was a slight structural effect in both of the protein complexes, which was controlled to be <10% by a fluorescence test [24].

2.2. Steady-state fluorescence measurements

A Fluorolog-3, ISA, Jobin-Yvon-Spex, Edison, NJ, was used to perform the emission spectral analysis of both protein-drug complexes, and the spectra recorded between 280 and 500 nm wavelengths with a 5 nm excitation, emission slit width. The emission spectra of both protein complexes were recorded at 298 K with 280 nm excitation, and we observed the maximum emission wavelengths at around 350 and 348 nm. Also, the τ_0 value for BSA 5.87 ns [13] and AChE 5.65 ns [25]. The decreasing fluorescence intensity of the BSA– and AChE– drug complex quenching mechanism determined using the Stern–Volmer equation. Also, the inner filter effect for the following steady-state spectrum was corrected [19].

2.3. Molecular docking

The selected ligand molecules (curcumin, piperine, silibinin and tacrine) were minimized by OPLS_2005 (Optimized Potentials for Liquid Simulations) force field using *Ligprep* application. Similarly, three-dimensional coordinates of crystal structure of AChE (PDB: 4EY6) [26] and BSA (PDB: 4F5S) [27] retrieved from the protein data bank. Then, the proteins were prepared [homo-dimer chain and crystallographic water molecules (beyond 4 Å) deleted and the hydrogen atoms, charges, formal bond orders and the missing residues were also added]. Further, restrained minimization has performed to relieve steric clashes using protein preparation wizard integrated in *Schrödinger software 11.2*, LLC [Maestro 2018]. The grid boxes generated over the ligand in the binding site of AChE and BSA of the reported structures which gives experimental evidence [26,28]. The Induced Fit Docking (IFD) process was used to refine the conformational flexibility of protein while ligand binding and the Extra Precision (XP) fixed scoring mode to gain exact energy [29]. All the above calculations have employed using the Schrödinger programme suite [Induced Fit docking protocol 2018]. The best ligand–protein complex identified based on the XP scoring and intermolecular interactions. We analyzed the intermolecular interactions between the ligand and protein using PyMol [30].

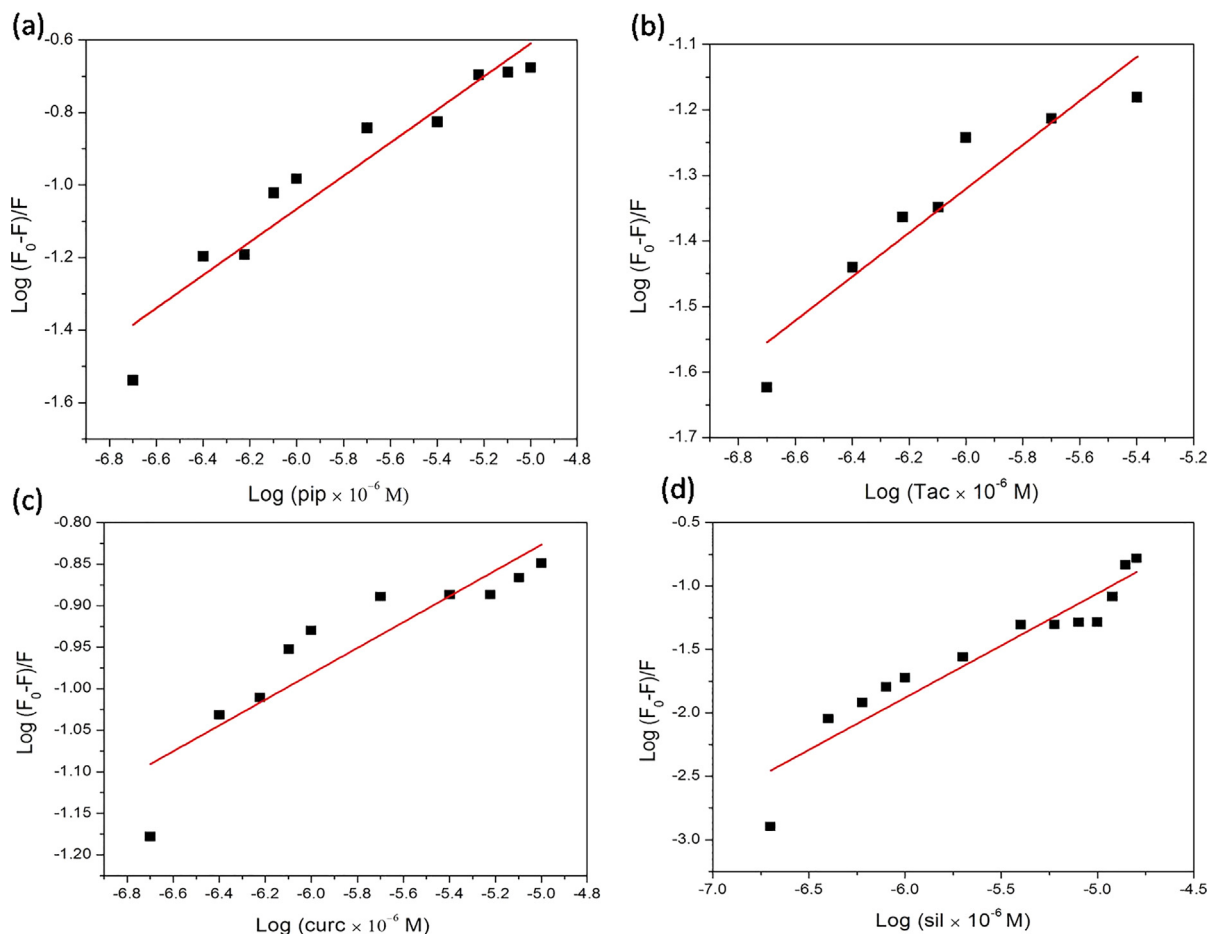


Fig. 4. Log plot of AChE with (a) Piperine (b) Tacrine (c) Curcumin (d) Silibinin complexes.

2.4. Molecular dynamics simulation

To explore the conformational changes, strength of ligand-protein interactions and properties of protein behavior, the energy surface was investigated by the way of solving Newton's laws of motion for the predicted system using physics-based modeling method of MD simulation approach. Before performing the MD simulation, the name of some residues has changed (GLU = GLH, Uncharged form; HIS = HID, δ -protonated form; ASP = ASH, Uncharged form and CYS = CYX, free form of disulfide bridge) because of the defined tautomeric or protonation states for the predicted residues. In the initial stages of MD simulation, it generated the atomic partial charges and MD parameters of ligand molecules with *gaff* force field using an *antechamber* program. In a similar fashion, the *AMBERff14SB* force field was used to construct the topological files for the AChE and BSA with the help of *tleap* module. In which, the counter-ions (Na^+) were placed to neutralize the entire system, and each system solvated in the orthorhombic shell of TIP3P water box with 9 Å distance of minimum solute-wall. Further, the two-stage of the pre-equilibration process (minimization) for both systems have performed using steepest descent and conjugate gradient methods; first, it relaxed the complex restrained with the native position and the solvents up to 10,000 steps, then continued up to 20,000 steps with no restrains. To achieve the annealing process with the maintenance of the canonical ensemble (NVT), we have heated the systems from 0 to 300 K at 200 ps time using the Langevin thermostat and Berendsen barostat. Finally, the MD production phase of each complex system was launched and

prolonged up to 40 ns in 2 fs time step with keeping isothermal-isobaric ensemble (NPT), constant temperature (300 K) and pressure (1 bar). The SHAKE and particle mesh Ewald (PME) algorithms were used to constrain the non-polar hydrogen atoms as well as to determine the electrostatic energy of the periodic box. The entire MD simulations of all the complexes have performed using *sander* routine in the AMBERTOOLS14 package [31]. To generate and analyze the MD trajectory with the help of XMGRACE, the VMD, CHIMERA and CPPTRAJ software's were used.

2.5. Binding free energy calculation

We estimated the binding affinities for all the complexes from the MM/PBSA and MM/GBSA methods. The MMPBSA.py routine was used to carry out all the above terms which are incorporated in AMBERTOOLS14 package [32,33]. Here, the enthalpy calculated using 2000 frames which are extracted from the 40 ns of MD trajectory. The contribution of non-polar desolvation computed with solvent accessible surface area (SASA) using the LCPO algorithm. Because of high computation, we have extracted 10 frames from every 4 ns trajectory. Further, to understand the nature of complex and ligand binding, the decomposition energy of each interaction was determined using MM/GBSA without the entropy contribution. The van der Waals and electrostatic interaction energies of intermolecular interactions present between ligand and each residue calculated. The ICOSA algorithm was used to predict the non-polar desolvation contribution.

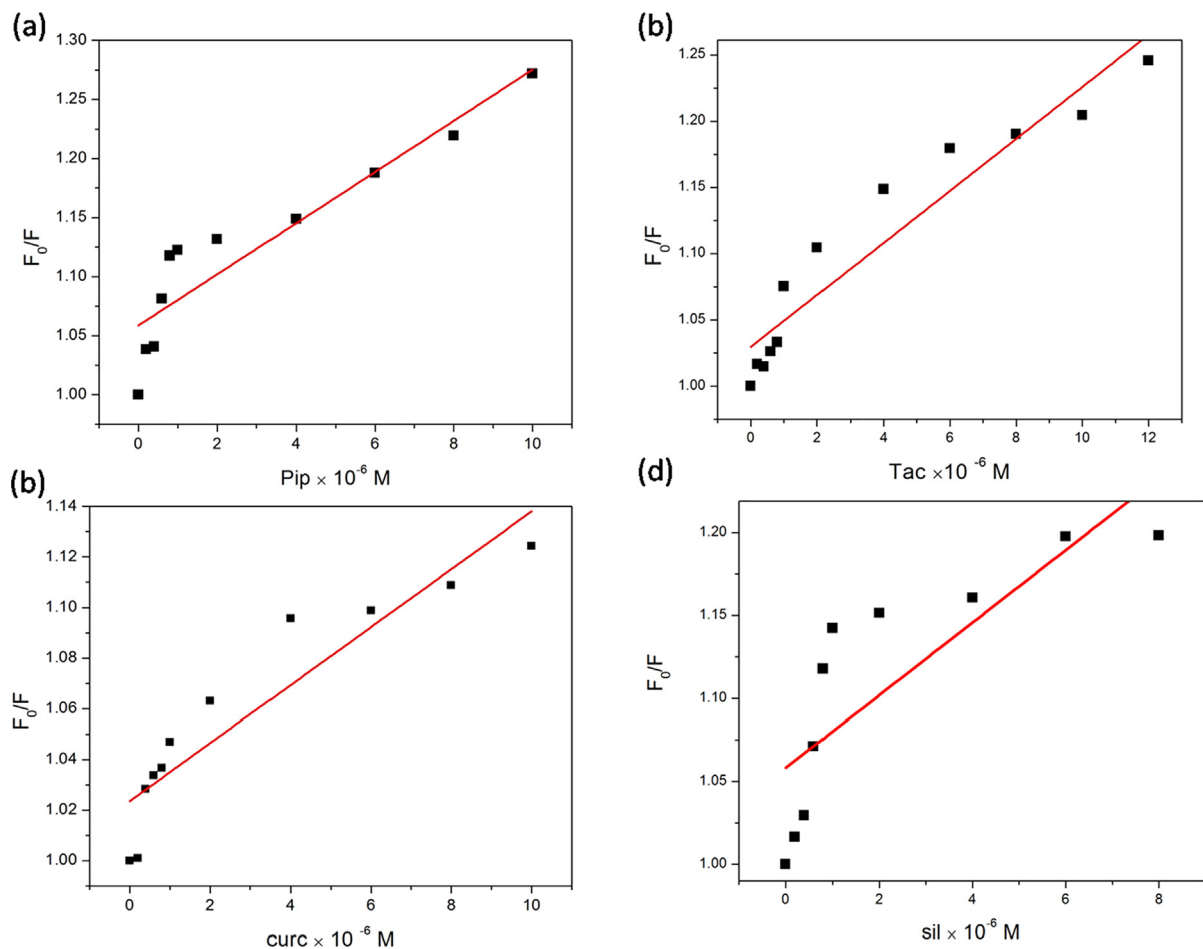


Fig. 5. Stern – Volmer plot of BSA with (a) Piperine (b) Tacrine (c) Curcumin (d) Silibinin complexes.

3. Results and discussion

3.1. Steady-state spectroscopy analysis

Steady state emission spectroscopy analysis is used to understand the drug quenching mechanism in the protein microenvironment. Figs. 1(a-d) and 2 (a-d) shows the fluorescence emission spectrum of bovine serum albumin (BSA) and AChE complex with (a) Piperine (b) Tacrine (c) Curcumin (d) Silibinin complexes. Initially the BSA, AChE molecules excited at 280 nm and the emission maximum is observed at 350 nm, 348 nm respectively. In Fig. 1 free BSA concentration is 10 μ M and drug concentration (a) piperine (0–10 μ M) (b) tacrine (0–12 μ M) (c) curcumin (0–10 μ M) (d) silibinin (0–8 μ M) with 1 μ M interval, and the Fig. 1 steady state emission spectrum result shows that the BSA maxima at 350 nm keeps on decreased without any further shift; while increasing the concentration of each drugs. In the case of AChE molecule shown in Fig. 2, the concentration of AChE is 10 μ M kept as constant and the drug concentration varies (a) piperine (0–2 μ M) (b) tacrine (0–1 μ M) (c) curcumin (0–1 μ M) (d) silibinin (0–4 μ M) with 0.2 μ M interval and the results shows decreased in AChE emission maxima without any shift. According to Figs. 1 & 2, these four drugs may form ground state complex in both protein molecules.

3.2. Quenching mechanism and number of binding sites

The fluorescence quenching results can reveal the information between protein and drug complex in detail. There are two types

of quenching which is defined as static and dynamic; The static quenching occur when the ground state complex is formed between protein and drug. For dynamic quenching the complex formation occurs between protein and drug during the excited state and it can be determined by using Stern –Volmer equation (1).

$$\frac{F_0}{F} = 1 + k_q \tau_0 [\text{drug}] = 1 + K_{SV} [\text{drug}] \quad (1)$$

Where F_0 and F refers to free protein molecule and drug molecule in protein complex. K_{sv} and K_q are Stern-Volmer binding and quenching constant respectively. τ_0 is life time value of protein molecule [12,13]. In general, many scientific reports [12,13] show that the maximum scatter collision K_q is $2.0 \times 10^{10} \text{ L mol}^{-1} \text{ s}^{-1}$. Table 1 represents the calculated quenching constant values of piperine, tacrine, curcumin, silibinin drugs in both BSA and AChE complex. According to that K_q value, piperine, tacrine, curcumin, silibinin drugs were binding static quenching mode in both protein molecules (Figs. 5 & 6). Also, the binding constant and number of binding sites calculated using the following equation (2)

$$\text{Log} \left[\frac{F_0 - F}{F} \right] = \text{Log} K_b + n \text{log} [\text{drug}] \quad (2)$$

Where K_b is the binding constant and n is the binding site between protein and drug, the calculated K_b was represented in table 1 and the number of binding sites was maintained at 1 during the binding process of piperine, tacrine, curcumin, silibinin drugs complex with both protein molecules (Figs. 3 & 4).

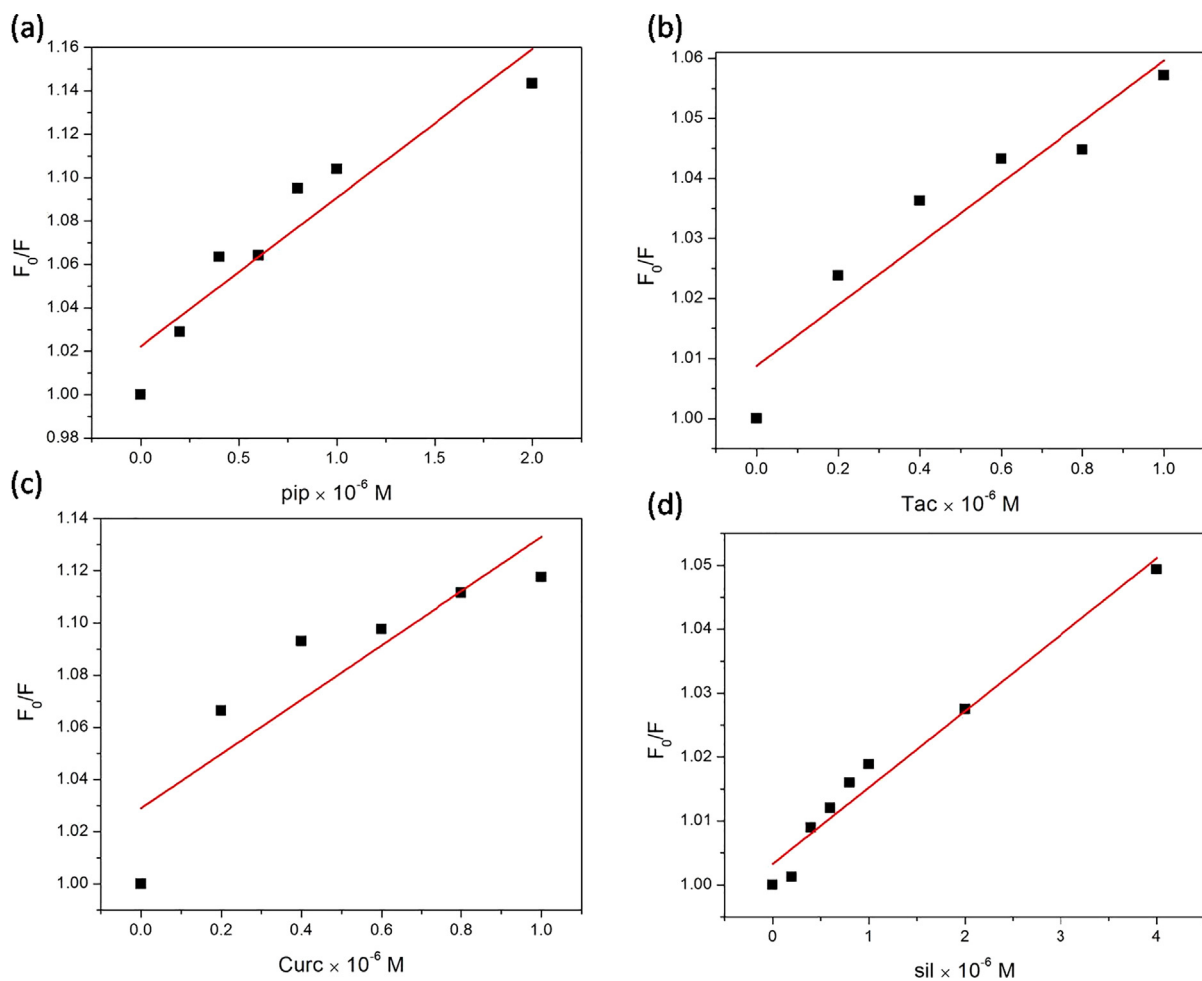


Fig. 6. Stern – Volmer plot of AChE with (a) Piperine (b) Tacrine (c) Curcumin (d) Silibinin complexes.

3.3. Excitation and emission matrix analysis

The three-dimensional fluorescence spectra will give total information relating to the fluorescence characteristics by dynamical excitation and emission wavelength simultaneously; so, it is a powerful methodology to review the conformational modification of protein complex. The excitation and emission matrix spectra of free BSA and BSA complex with piperine, curcumin, silibinin drugs is shown in Fig. 7, also free AChE and AChE complex with piperine, tacrine, curcumin, silibinin drugs shown in Fig. 8. As shown in Figs. 7a and 8a is represents the image free BSA (10 μ M) and AChE (10 μ M) protein molecule due to the TRP and TYR residues. It could be noted that in both Figs. 7 & 8 (b-e) (10 μ M) while increasing the concentration of the drug, there is a clear decrease in emission maximum without any shift and this result suggest that piperine, tacrine, curcumin, silibinin drugs ground state complex formation in both BSA, AChE protein molecule.

3.4. Intermolecular interaction

To identify the plausible binding mode of chosen ligand molecules with the active site of AChE and BSA, we analyzed the molecular docking. The lowest binding energy (Glide energy) of the curcumin, piperine, silibinin and tacrine with AChE got from docking analysis are -12.97 , -11.24 , -15.72 and -6.20 kcal/mol respectively. Based on the docking results, silibinin exhibits the lowest

energy and high binding affinity towards AChE. The intermolecular interactions of the selected molecules with AChE are shown in Figure S1. In the curcumin-AChE complex, curcumin forms hydrogen bonding with Glu202, Tyr133 and Tyr337; in the piperine-AChE complex, we observed hydrogen bond between piperine and Phe295/Arg296, the same interactions also found in the silibinin-AChE. In the silibinin-AChE complex, the oxygen atoms in the flavanone group are forming strong hydrogen bonding interaction with the catalytic site amino acids Ser203 and His447 at the distance 2.7 and 2.5 \AA respectively. Notably, the π - π stacking was also noticed between Try86/His447 and curcumin/silibinin/tacrine. Moreover, the catalytic amino acid Ser203 forms water mediated hydrogen bond in these complexes [22,23]. Whereas in the curcumin, piperine, silibinin and tacrine with BSA complexes, the glide energy values are -85.22 , -61.14 , -90.95 and -39.42 kcal/mol. The intermolecular interactions of BSA-ligand complexes are shown in Fig. 9. All the molecules located and formed strong intermolecular interactions with the drug binding site I (domain IIA) region of BSA. In the curcumin-BSA complex, the keto-enol group of curcumin is forming strong hydrogen bonding with Ala209 and Val481, the distances are 2.0 and 2.2 \AA respectively. The curcumin molecule also forms π cation interaction with Lys350 and π π interaction with Trp213. In the piperine-BSA complex, the residue Lys350 makes H-bond interaction with keto group of piperine and Trp213 makes π π interaction with the 5-membered ring. In the silibinin-BSA complex, the hydroxyl group of silibinin molecule forms H-bond with Arg194, Arg208, Leu326 and Ser343, the dis-

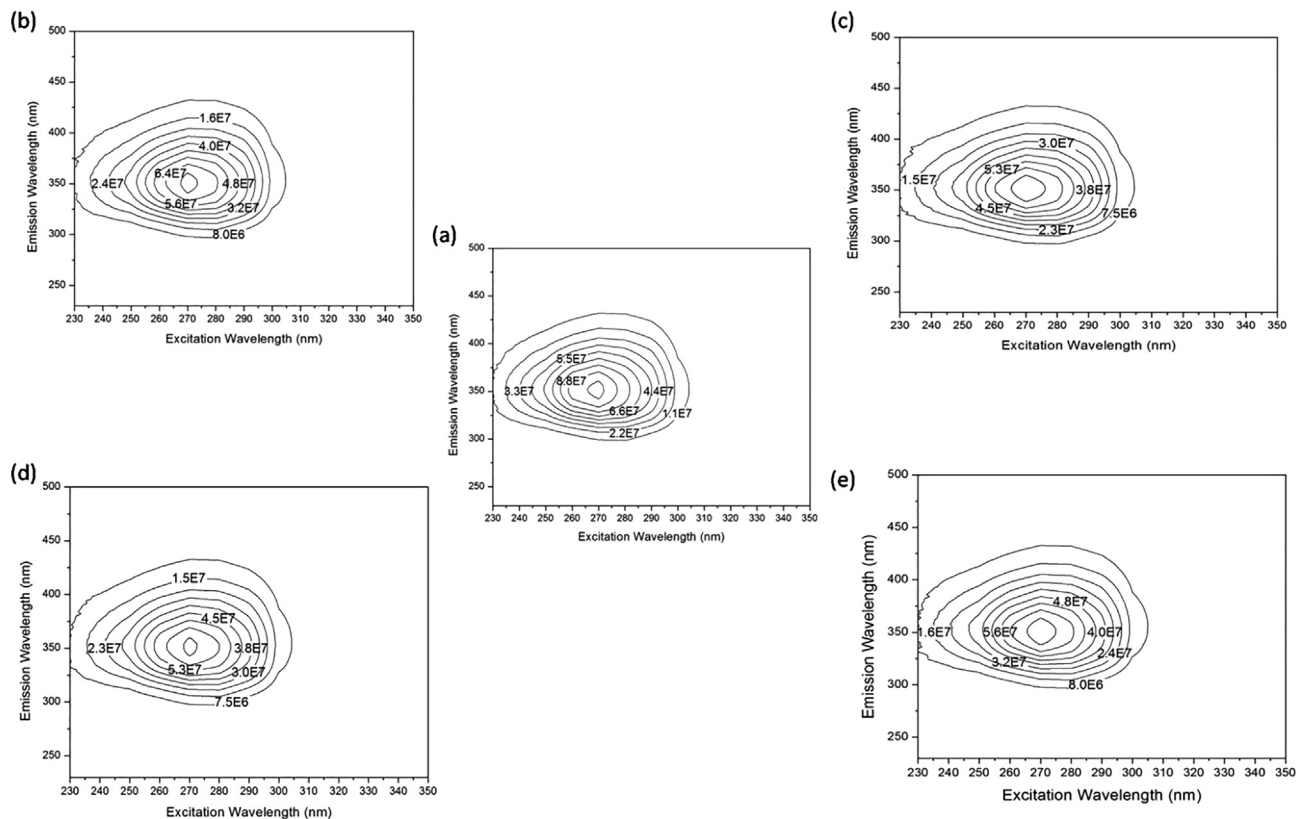


Fig. 7. Excitation emission matrix analysis of BSA with (a) Piperine (b) Tacrine (c) Curcumin (d) Silibinin complexes.

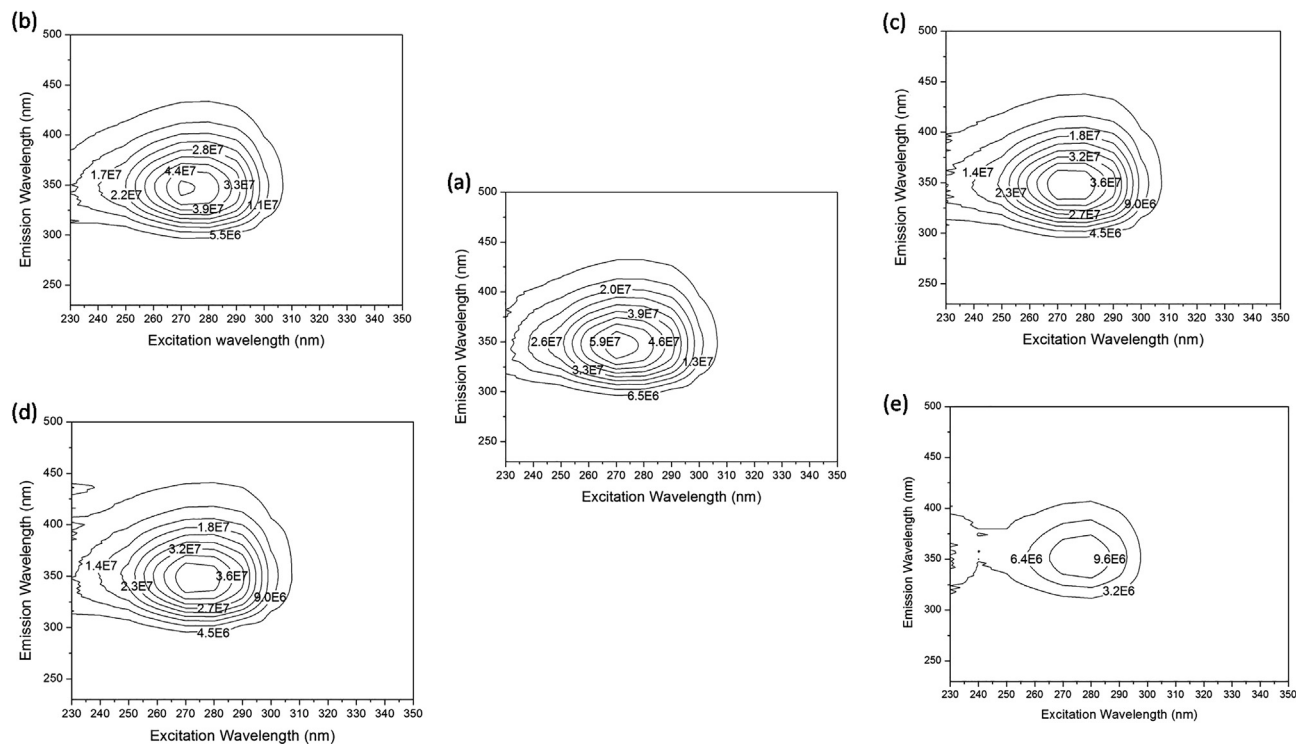


Fig. 8. Excitation emission matrix analysis of AChE with (a) Piperine (b) Tacrine (c) Curcumin (d) Silibinin complexes.

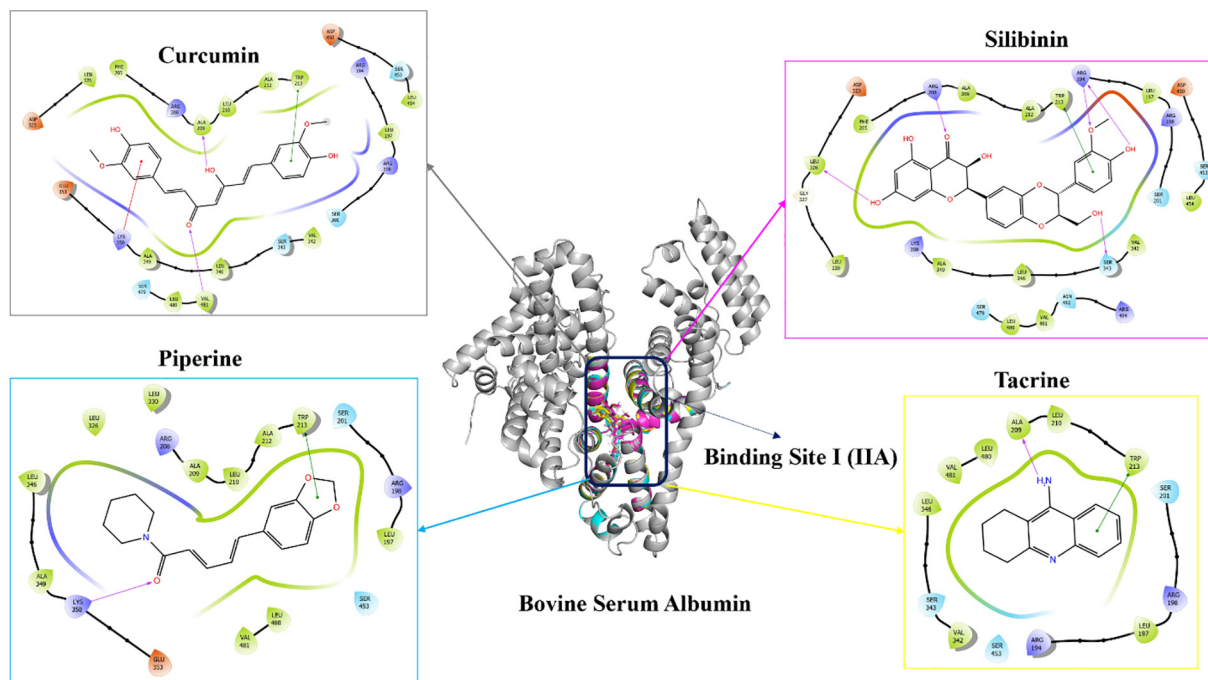


Fig. 9. Intermolecular interactions in 2D view of all the four molecules with BSA.

tances are 2.3, 2.5, 2.2 and 2.2 Å respectively. The π – π interactions observed between silibinin and Trp213. In the tacrine-BSA complex, the Ala209 forms a hydrogen bond (2.1 Å) and Trp213 forms π – π interaction. The figure (Fig. 9) displays several hydrophobic interactions with the drug binding I region and Trp213 makes π – π interaction with all the ligand molecules which confirms the binding similarity with fluorescence results.

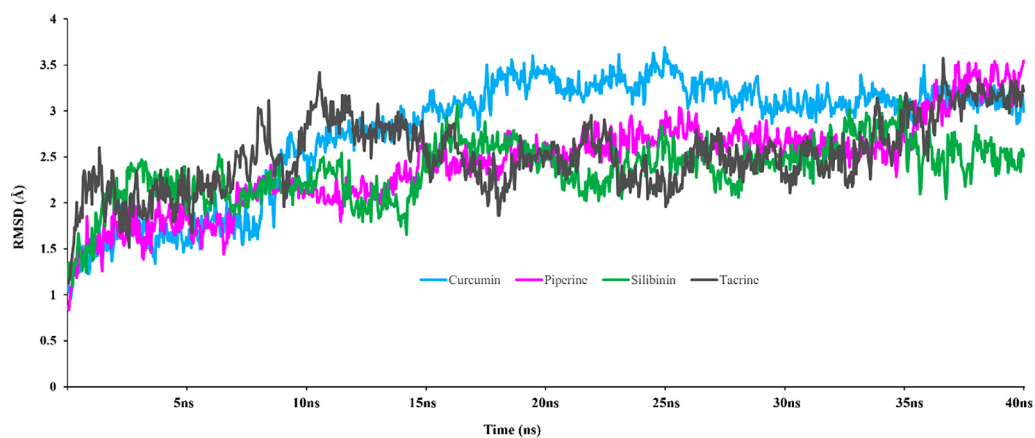
3.5. RMSD, RMSF and radius of gyration

Molecular docking is one of the testimonies with the highest docking score; the ligand molecule may fly away from the active site of protein in the physiological condition. Hence, the MD simulation is trustful tool to validate as well as to study the interactions at microscopy level between protein and ligands to identify the potent inhibitor. Therefore, we have performed the MD simulation for all the complexes (AChE/BSA – curcumin/piperine/silibinin/tacrine) to understand the conformation, stability and binding free energy. The statistical parameters of these complexes are calculated from initial coordinates to understand the deviation (RMSD), fluctuation (RMSF) and compactness (Rg) of these complexes (Fig. 10 & Fig. S2). **In the BSA-ligands:** On comparing the RMSD of all four complexes, it falls between ~0.91 to 3.42 Å. The deviations of all the C α and backbone atoms are small and that confirms these complexes are highly stable during MD simulation. Notably, the silibinin-BSA complex (<2.5 Å) is highly stable than the other complexes. From the RMSF, we have found a large fluctuation in the loop regions and the fluctuation is very less in the active site regions. And, the RMSF of N-terminal region is higher than the C-terminal because the N-terminal region has a long looped region and conformationally fluctuated by the influence of ligand molecules. The radius of gyration (Rg) of the BSA-ligand complexes calculated and plotted; the average Rg values are ~20.25 Å. This confirms ligand molecules in the binding site is not much affects

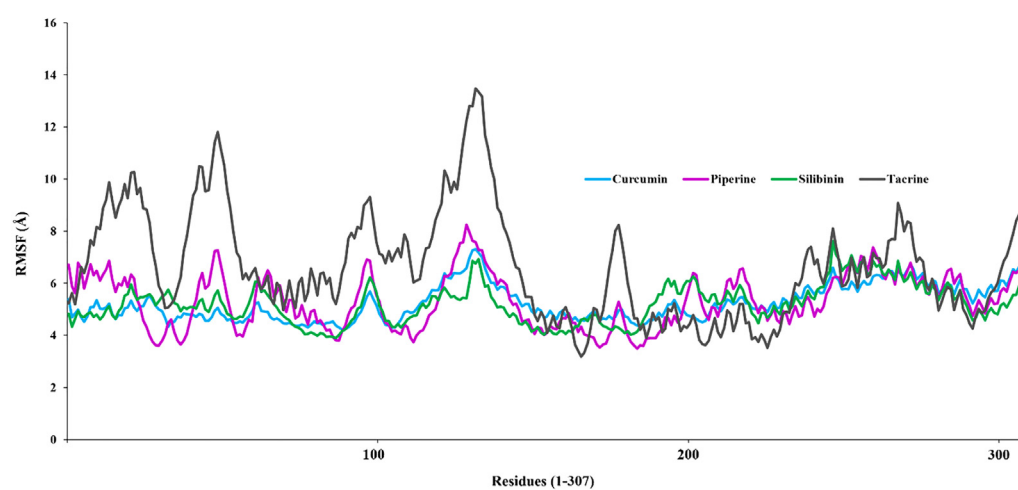
the compactness of BSA. **In the AChE-ligands,** Fig. S2 shows the observed RMSD of the four complexes which exhibit an equilibrium state. On comparing the RMSD of these complexes, the RMSD of the silibinin-AChE complex slightly higher than the other complexes, falls on between ~2.0 to 2.5 Å and the other three complexes are ~1.0 to 2.0 Å. In the curcumin-AChE complex, RMSD has deviated after 30 ns; then, it becomes stable up to 40 ns. The RMSF of the four complexes was observed; in which, the large fluctuation has noticed in the loop regions, N and C-terminals due to the influence of ligand molecules. The active site regions are lesser fluctuated than other parts of the protein; notably, the RMSF of catalytic site amino acids Ser203 and His447 are less than 1 Å. After the MD simulation, intermolecular interactions were analyzed; in which, the catalytic site amino acid Ser203 maintains strong interaction with curcumin. And, Trp86, Glu202 and Phe295 as keeps maintaining their interactions with tacrine, piperine, silibinin.

3.6. Binding free energy

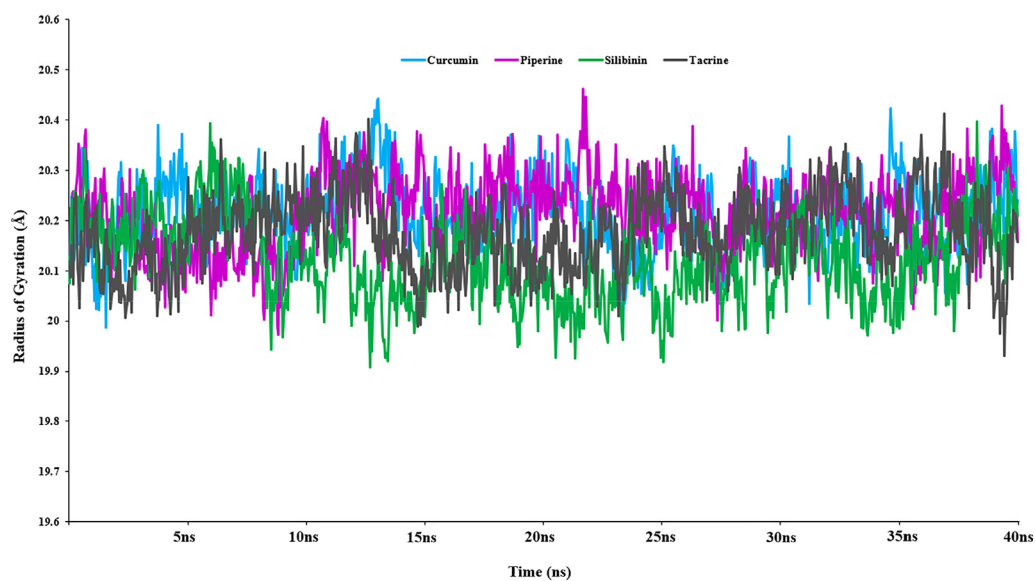
To determine the detailed energy contribution based on Molecular Generalized Born/ Poisson-Boltzmann Surface Area (MM-GBSA/MM-PBSA) approaches, the binding free energies of all the selected complexes were calculated from the MD simulation. In this calculation, several energy components are included in the binding energy such as van der Waals, electrostatic energy, polar and non-polar solvation free energy. The detailed binding free energies of BSA-ligand complexes are summarized in Table 2. In which the silibinin-BSA complex shows high binding energy (–60.94 kcal/mol) than other complexes. From these binding studies, we can conclude that all the molecules exhibit strong interactions with BSA in the following [silibinin > curcumin > piperine > tacrine] order. Whereas, the binding free energy of AChE-ligand complexes are –77.519 (curcumin), –37.732 (piperine), –79.053 (silibinin) and –52.169 (tacrine) kcal/mol, the order



(a)



(b)



(c)

Fig. 10. Statistical parameters (a) RMSD, (b) RMSF and (c) Rg of four molecules with BSA.

Table 2

Contributions of various energy components to the binding free energy (kcal/mol) for the selected molecule-BSA complexes.

	Curcumin	Piperine	Silibinin	Tacrine
ΔE_{vdw}	-52.17 (± 2.73)	-42.91 (± 2.54)	-65.80 (± 3.18)	-31.89 (± 2.22)
$\Delta E_{\text{electrostatic}}$	-20.36 (± 6.88)	-10.98 (± 3.26)	-41.41 (± 6.46)	-8.46 (± 5.21)
ΔG_{GB}	38.63 (± 3.92)	22.42 (± 2.79)	54.68 (± 4.14)	17.62 (± 3.95)
ΔG_{PB}	48.59 (± 4.66)	30.98 (± 2.20)	63.48 (± 4.51)	25.02 (± 3.97)
$\Delta G_{\text{SA-GB}}$	-7.6 (± 0.19)	-5.89 (± 0.17)	-8.40 (± 0.18)	-3.83 (± 0.15)
$\Delta G_{\text{SA-PB}}$	-4.84 (± 0.10)	-3.88 (± 0.07)	-5.33 (± 0.10)	-2.87 (± 0.06)
$\Delta E_{\text{gas}} (E_{\text{MM}})$	-72.53 (± 6.41)	-53.89 (± 3.85)	-107.21 (± 6.01)	-40.36 (± 4.52)
$\Delta G_{\text{sol-GB}}$	31.03 (± 3.92)	16.53 (± 2.23)	46.27 (± 4.18)	13.78 (± 4.01)
$\Delta G_{\text{sol-PB}}$	43.75 (± 4.65)	27.09 (± 2.21)	58.14 (± 4.51)	22.14 (± 3.97)
$\Delta G_{\text{total-GB}}$	-41.50 (± 3.53)	-37.36 (± 3.38)	-60.94 (± 3.62)	-26.57 (± 2.53)
$\Delta G_{\text{total-PB}}$	-28.78 (± 3.75)	-26.79 (± 3.47)	-49.06 (± 4.13)	-18.21 (± 3.10)

is silibinin > curcumin > tacrine > piperine. Further, the decomposition energy of the important residues carried out to understand the binding mechanism of the complexes. In which, the decomposition energy of binding site I residues which is forming hydrogen bonding with ligand molecules are carrying ~ 5 kcal/mol; however, Trp213 forms hydrophobic interaction which exhibits higher decomposition energy (~4kcal/mol in all for complexes) than other binding site residues [33–35]. This result clearly shows that these molecules are strongly interacting with binding site I of BSA.

3.7. Non-covalent interaction (NCI) analysis

To quantify intermolecular contacts and visualize the contacts between ligand and active site residues, Hirshfeld surface with fingerprint plots calculated for curcumin, piperine, silibinin and tacrine - AChE/BSA complexes using *Crystal Explorer 17.5* [36]. Hirshfeld surface is defined by the density weight function of the selected molecule over the same sum of the density of its nearest molecule, which can map with unique properties like d_{norm} , electrostatic potential, shape-index and curvedness. These are useful to accumulate additional information on weak intermolecular interactions. The d_{norm} of Hirshfeld surfaces map use the function of normalized distances of both the distances from the surface to the nearest atom outside and inside (d_{e} and d_{i}). The figure (Fig. 11 & Fig. S3) shows the d_{norm} map of protein-ligand complexes; in which, the red, white and blue surface denotes hydrogen bonding interactions, vdW separation and short contact distances, respectively. It confirms the corresponding fingerprint plots of these complexes, the hydrogen bonding from sharp spikes.

To understand the binding mechanism of protein-ligand complexes, non-covalent interaction energy calculation has performed using Gaussian-based quantum mechanical platforms. The intermolecular interaction energies of each active site amino acid of BSA and AChE with curcumin, piperine, silibinin and tacrine were calculated with B3LYP/6-311G** by *Gaussian 09* software [37]. On comparing the interaction energy of all the pair-wise molecules, the Lys350 of BSA carries higher interaction energy with the piperine molecule than the other interactions, the value is -15.000 kcal/mol. The wave function of the corresponding interaction has submitted into *Multiwfn* software to get the reduced density gradient (RDG) and its isosurface [38]. RDG is $S(r)$, used to find the presence of non-covalent interaction in low electron density region, defined as

$$S(r) = \frac{|\nabla\rho(r)|}{2(3\pi^2)^{\frac{1}{3}}\rho(r)^{\frac{4}{3}}} \quad (3)$$

Where, the gradient of electron density at the point r is $\nabla\rho(r)$. It shows the RDG scatter plot of Lys350 of BSA with piperine in Figure. In which, the blue region shows strong interactions (hydrogen bonding), the green region displays the van der Waals interactions and the red region reflects the steric effect in the ring. Notably, RDG isosurface shows a different type of interaction on their strength. To calculate the RDG of electron density, the electron density grids for the strong interactions between BSA and curcumin/piperine/silibinin/tacrine created using *VMOPro* and then visualized these NCI isosurface in by *Mollso* software [39,40]. The figure (Fig. 12 & Fig. S4) shows the 3D isosurface map of selected interactions between AChE/BSA-ligand complexes; in which, the shape of the isosurface was confirmed the strong interactions from the vicinity of isosurface got between protein and ligand.

4. Summary and conclusion

In the summary of the present study, the interaction steady from fluorescence spectroscopy (fluorescence emission, quenching, excitation-emission matrix) was analyzed for the selected protein-ligand complexes. In the overall fluorescence study, the results suggest the presence of piperine, tacrine, curcumin, silibinin molecules in both BSA and AChE complex with static quenching mode. From the computational analysis, the molecular docking study confirms all the molecules are forming strong interactions with the binding site I of BSA and AChE. MD simulation confirms the stability of ligand molecules in the active site of both BSA and AChE during the dynamical behavior. Besides, the free energy (ΔG) change from the MM-PB/GBSA free energy calculation has been almost the same order as the thermodynamic calculation. Hirshfeld surface analysis has been carried out to examine the intermolecular interactions between protein and ligands. The residual density gradient of non-covalent interaction supports the existence of weak interactions in the protein-ligand complexes. These results show that the current comparative calculations completely reproduce the experimental results and provide interesting evidence for the already known molecules. The results not only well explain the interaction mechanisms between BSA and AChE, but also provide substantial information for better understanding the molecules.

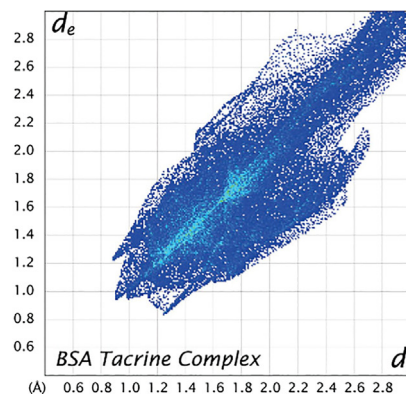
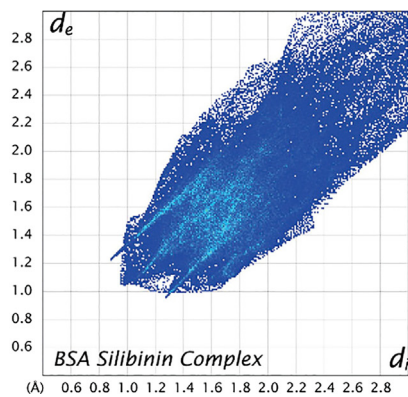
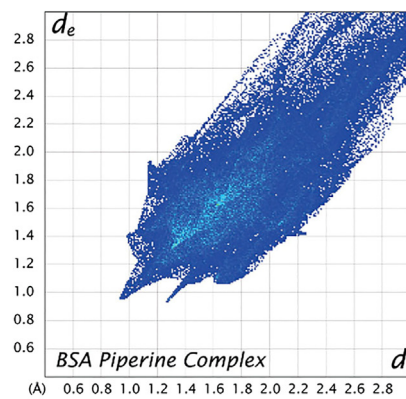
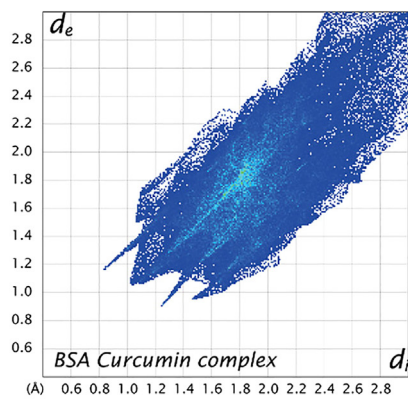
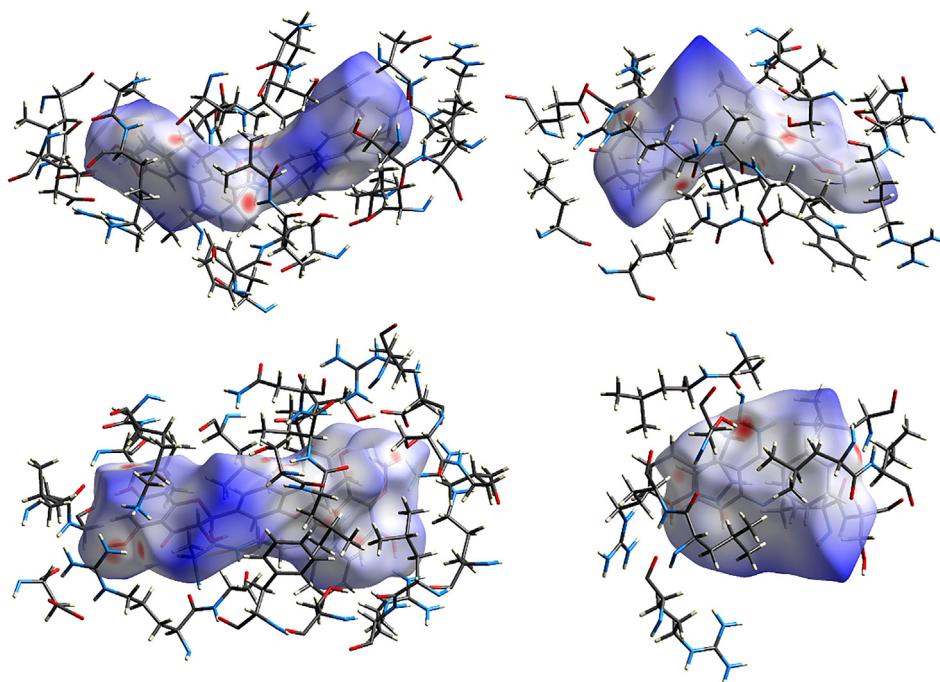


Fig. 11. Hirshfeld Surface analysis with corresponding 2D fingerprint map of protein-ligand complexes, (a) d_{norm} map of BSA with curcumin (1), piperine (2), silibinin (3) and tacrine (4).

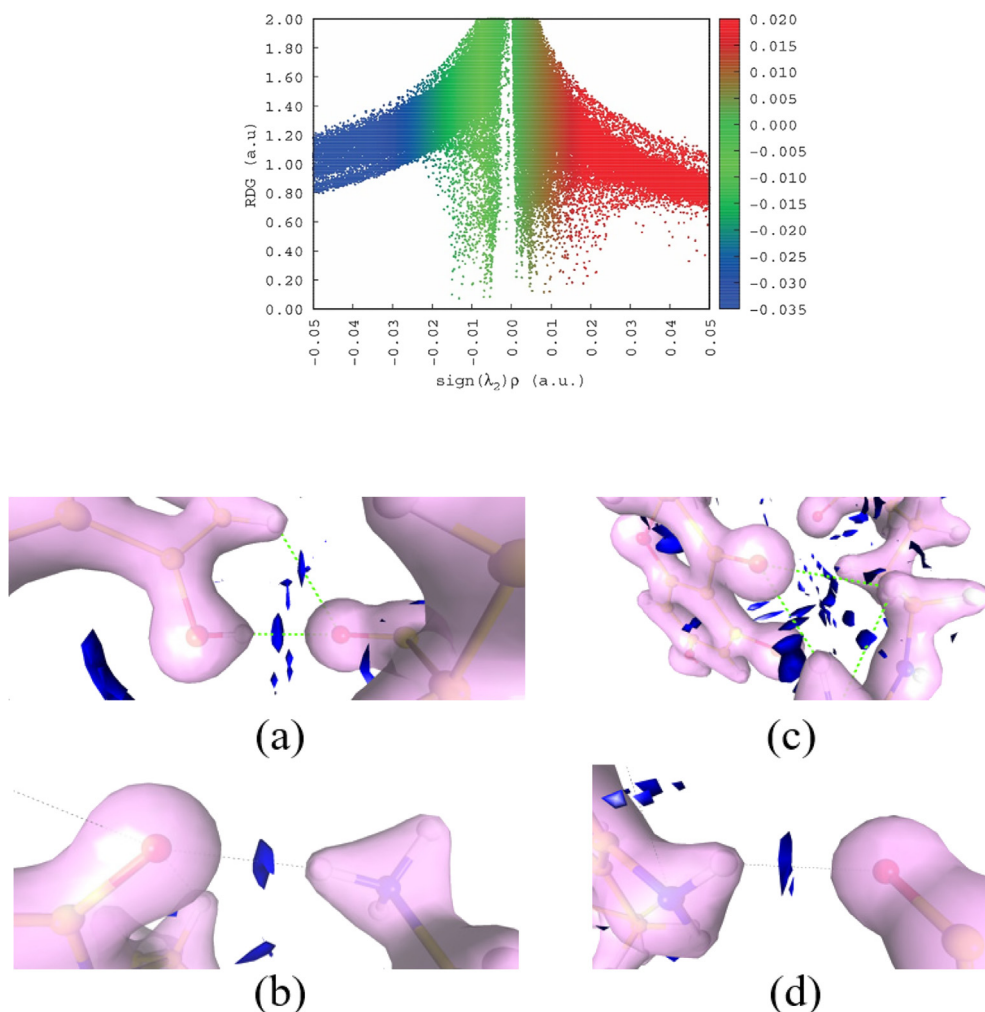


Fig. 12. RDG scatter plot of Lys350 of BSA with piperine and NCI Isosurface plot for the Ala209 with curcumin (a), Lys350 of BSA with piperine (b), Arg194 of BSA with silibinin (c) and Ala209 of BSA with tacrine (c).

CRediT authorship contribution statement

Kandasamy Saravanan: Writing - original draft, Methodology, Validation. **Subramani Karthikeyan:** Formal analysis, Data curation. **Srinivasan Sugarthi:** Formal analysis. **Arputharaj David Stephen:** Formal analysis.

Declaration of Competing Interest

The authors declare that they have no known competing financial interests or personal relationships that could have appeared to influence the work reported in this paper.

Appendix A. Supplementary material

Supplementary data to this article can be found online at <https://doi.org/10.1016/j.saa.2021.119856>.

References

- [1] A. Association, 2017 Alzheimer's disease facts and figures, *Alzheimer's Dementia* 13 (4) (2017) 325–373.
- [2] I.O. Korolev, Alzheimer's disease: a clinical and basic science review, *Int. J. Alzheimer's Dis.* 4 (2014) 24e33.
- [3] A. Contestabile, The history of the cholinergic hypothesis, *Behav. Brain Res.* 221 (2011) 334–340.
- [4] D. Casey, D. Antimisariaris, J. O'Brien, Drugs for Alzheimer's disease: are they effective?, *P.T.* 35 (2010) 208–211.
- [5] K.G. Yiannopoulou, S.G. Papageorgiou, Current and future treatments for Alzheimer's disease, *Ther. Adv. Neurol. Disord.* 6 (2013) 19–33.
- [6] G. Natalia, W. Anna, P. Dawid, M. Barbara, Recent development of multifunctional agents as potential drug candidates for the treatment of Alzheimer's disease, *Cur. Med. Chem.* 22 (2015) 373–404.
- [7] L. Calcul, B. Zhang, U.K. Jinwal, C.A. Dickey, B.J. Baker, Natural products as a rich source of tau-targeting drugs for Alzheimer's disease, *Future Med. Chem.* 4 (2012) 1751–1761.
- [8] T.S. Anekonda, P.H. Reddy, Can herbs provide a new generation of drugs for treating Alzheimer's disease?, *Brain Res. Rev.* 50 (2005) 361–376.
- [9] K.A. Majorek, A. Karolina, et al., Structural and immunologic characterization of bovine, horse, and rabbit serum albumins, *Mol. Immunol.* 52 (3–4) (2012) 174–182.
- [10] X.M. He, D.C. Carter, Atomic structure and chemistry of human serum albumin, *Nature* 358 (1992) 209–215.
- [11] G. Rabbani, S.N. Ahn, Structure, enzymatic activities, glycation and therapeutic potential of human serum albumin: a natural cargo, *Int. J. Biol. Macromol.* 123 (2019) 979–990.
- [12] S. Karthikeyan et al., Comparative binding analysis of N-acetylneuraminic acid in bovine serum albumin and human α -1 acid glycoprotein, *J. Chem. Inform. Model.* 59 (1) (2018) 326–338.
- [13] S. Karthikeyan et al., Exploring the binding interaction mechanism of taxol in β -tubulin and bovine serum albumin: a biophysical approach, *Mol. Pharm.* 16 (2) (2019) 669–681.
- [14] R. Kannan, K. Ponnusamy, S. Chellappan, Excitation-resolved area-normalized emission spectroscopy: a rapid and simple steady-state technique for the analysis of heterogeneous fluorescence, *RSC Adv.* 10 (2) (2020) 998–1006.
- [15] P. Chonpathompikunlert, J. Wattanathorn, S. Muchimapura, Piperine, the main alkaloid of Thai black pepper, protects against neurodegeneration and cognitive impairment in animal model of cognitive deficit like condition of Alzheimer's disease, *Food Chem. Toxicol.* 48 (2010) 798e802.

- [16] T. Esatbeyoglu, Tuba, et al., Curcumin—from molecule to biological function, *Angew. Chem. Int. Ed.* 51 (22) (2012) 5308–5332.
- [17] P. Kidd, H. Kathleen, A review of the bioavailability and clinical efficacy of milk thistle phytosome: a silybin-phosphatidylcholine complex (Siliphos), *Altern. Med. Rev.* 10 (2005) 3.
- [18] N. Qizilbash et al., Cholinesterase inhibition for Alzheimer disease: a meta-analysis of the tacrine trials, *JAMA* 280 (20) (1998) 1777–1782.
- [19] A.S.A. Manap, A.C.W. Tan, W.H. Leong, et al., Synergistic effects of curcumin and piperine as potent acetylcholine and amyloidogenic inhibitors with significant neuroprotective activity in SH-SY5Y cells via computational molecular modeling and in vitro assay, *Front. Aging Neurosci.*, 11 (2019).
- [20] S. Duan, X. Guan, R. Lin, X. Liu, Y. Yan, R. Lin, H. Gu, Silibinin inhibits acetylcholinesterase activity and amyloid β peptide aggregation: a dual-target drug for the treatment of Alzheimer's disease, *Neurobiol. Aging* 36 (5) (2015) 1792–1807.
- [21] V. Tumiatti, A. Minarini, M.L. Bolognesi, A. Milelli, M. Rosini, C. Melchiorre, Tacrine derivatives and Alzheimer's disease, *Curr. Med. Chem.* 17 (17) (2010) 1825–1838.
- [22] K. Saravanan, C. Kalaiarasi, P. Kumaradhas, Understanding the conformational flexibility and electrostatic properties of curcumin in the active site of rhAChE via molecular docking, molecular dynamics, and charge density analysis, *J. Biomol. Struct. Dyn.* 35 (2017) 3627–3647.
- [23] K. Saravanan et al., Exploring the different environments effect of piperine via combined crystallographic, QM/MM and molecular dynamics simulation study, *J. Mol. Graph. Model.* 92 (2019) 280–295.
- [24] M.G. Corradini, M. Demol, J. Boeve, et al., Fluorescence spectroscopy as a tool to unravel the dynamics of protein nanoparticle formation by liquid antisolvent precipitation, *Food Biophys.* 12 (2017) 211–221, <https://doi.org/10.1007/s11483-017-9477-4>.
- [25] Jyoti Korram, Lakshita Dewangan, Indrapal Karbhal, Rekha Nagwanshi, Sandeep K. Vaishnav, Kallol K. Ghosh, Manmohan L. Satnami, CdTe QD-based inhibition and reactivation assay of acetylcholinesterase for the detection of organophosphorus pesticides, *RSC Adv.* 10 (2020) 24190–24202.
- [26] J. Cheung et al., Structures of human acetylcholinesterase in complex with pharmacologically important ligands, *J. Med. Chem.* 55 (22) (2012) 10282–10286.
- [27] A. Bujacz, Structures of bovine, equine and leporine serum albumin, *Acta Crystallogr. Sect. D: Biol. Crystallogr.* 68 (10) (2012) 1278–1289.
- [28] R. Castagna, S. Donini, P. Colnago, A. Serafini, E. Parisini, C. Bertarelli, Biohybrid electrospun membrane for the filtration of ketoprofen drug from water, *ACS Omega* 4 (8) (2019) 13270–13278.
- [29] Induced Fit docking protocol, Small-molecular Drug Discovery suite 2014-2 version 6.3, Schrodinger, LLC, New York, 2014.
- [30] W.L. DeLano, PyMol molecular graphics system, DeLano Scientific, San Carlos, CA, USA, 2002.
- [31] D.A. Case et al., AMBER 14, University of California, San Francisco, 2014.
- [32] B.R. Miller, T.D. McGee, J.M. Swails, N. Homeyer, H. Gohlke, A.E. Roitberg, MMPBSA.py: an efficient program for end-state free energy calculation, *J. Chem. Theory Comput.* 8 (2012) 3314e3321.
- [33] K. Saravanan, M. Sivanandam, G. Hunday, L. Mathiyalagan, P. Kumaradhas, Investigation of intermolecular interactions and stability of verubecestat in the active site of BACE1: development of first model from QM/MM based charge density and MD analysis, *J. Biomol. Struct. Dyn.* 36 (2018) 1–16.
- [34] K. Saravanan, P. Kumaradhas, Acylguanidine-BACE1 complex: Insights of intermolecular interactions and dynamics, *J. Theo. Bio.* 464 (2019) 33–49.
- [35] K. Saravanan, G. Hunday, P. Kumaradhas, Binding and stability of indirubin-3-monoxime in the GSK3 β enzyme: a molecular dynamics simulation and binding free energy study, *J. Biomol. Struct. Dyn.* 37 (2019) 1–18.
- [36] CrystalExplorer (Version17.5), S.K. Wolff, D.J. Grimwood, J.J. McKinnon, M.J. Turner, D. Jayatilaka, M.A. Spackman, University of Western Australia, 2012.
- [37] M.J. Frisch, G.W. Trucks, H.B. Schlegel, et al. Gaussian 09, Revision A.02, Gaussian, Inc., Wallingford CT, 2016.
- [38] T. Lu, F. Chen, Multiwfn: a multifunctional wavefunction analyzer, *J. Comput. Chem.* 33 (5) (2012) 580–592.
- [39] C. Jelsch, B. Guillot, A. Lagoutte, C. Lecomte, Advances in protein and small-molecule charge-density refinement methods using MoPro, *J. Appl. Crystallogr.* 38 (1) (2005) 38–54.
- [40] C.B. Hübschle, P. Luger, Mollso—a program for colour-mapped iso-surfaces, *J. Appl. Crystallogr.* 39 (6) (2006) 901–904.